Original Article

Institution of MECHANICAL ENGINEERS
Journal of MECHANICAL ENGINEERING SCIENCE

Proc IMechE Part C:
J Mechanical Engineering Science
0(0) 1–14

DOI: 10.1177/0954406215602035
pic.sagepub.com
SAGE

Modeling the constraint effects of compliant electrodes in dielectric elastomers under uniaxial loading

Heather L Lai[1] and Chin An Tan[2,3]

Abstract

Dielectric elastomers are composite thin film structures composed of a dielectric polymer between compliant electrodes. Previous hyperelastic models have not modeled the constraint effects of compliant electrodes on the lateral contraction of the dielectric material as it stretches, and are therefore unable to fully describe the electromechanical behavior of the dielectric elastomer or provide a means to understand the constraint effects. An empirical boundary coefficient is introduced to model these constraint effects on the lateral boundaries of the material under uniaxial tension. Employing an averaged stretch ratio concept, it is shown that this coefficient can be obtained from experimentally measurable geometric variables. Values for the boundary coefficients of sample dielectric elastomer films were obtained from experiments performed on a uniaxial test stand. Incorporating the boundary coefficient into the model formulation, a specific hyperelastic stress–strain relation is derived to describe the electromechanical behavior of dielectric elastomers under combined uniaxial tension and electrical loading. Comparison of the experimental and predicted values of the induced force in the axial direction due to the Maxwell stress based on the uniaxial model shows favorable agreement.

Keywords

Dielectric elastomer, composite thin film structure, compliant electrode, kinematic constraints, hyperelastic, boundary coefficient, Maxwell stress, electrostatic

Date received: 22 January 2015; accepted: 16 July 2015

Introduction

Electroactive polymers (EAP) are soft functional materials that exhibit a change in size or shape when stimulated by an electric field, and can undergo a large amount of deformation.[1] Over the last decade, there have been significant advances in developing these materials as actuators and sensors for a broad spectrum of applications.[2–4] While individual devices made of these materials can vary substantially, the electromechanical coupling within the EAP allows conversion between the mechanical strain energy and the electrical energy. This mechanism provides a means to produce a soft, comfortable material which can be controlled to perform not only sensing and actuation, but energy harvesting as well.[5–7]

Dielectric elastomers (DE), one type of EAP, are composite thin film structures composed of a dielectric polymer sandwiched by compliant electrodes, forming a variable capacitance device. These are extremely elastic materials capable of strains exceeding 100% elongation and are electromechanically coupled through an electrostatic effect.[8] Examples of dielectric polymers are acrylic and silicone,[7] while electrode materials currently used in DE applications include carbon grease,[9] graphene,[10,11] silver,[12–14] and corrugated metal.[15,16] By exposing this elastomer capacitor to an electric field, an electrostatic stress (Maxwell stress) is induced, causing the elastomer to experience a mechanical strain. The capacitance of two electrode surfaces separated by a dielectric depends not only on the permittivity of the dielectric, but also on the surface area and thickness of the dielectric; therefore the capacitance is a function of the geometry of the device and is directly affected by the material properties and strains. This variation of capacitance due to mechanical strain provides a

[1]Department of Biomedical Engineering, Wayne State University, Detroit, MI, USA
[2]Department of Mechanical Engineering, Wayne State University, Detroit, MI, USA
[3]Affiliated with Sound and Vibration Laboratory, College of Mechanical Engineering, Zhejiang University of Technology, Hangzhou, China

Corresponding author:
Heather L Lai, Department of Biomedical Engineering, Wayne State University, 818 W Hancock Street, Detroit, MI 48201, USA.
Email: heather.lai@wayne.edu

means for converting mechanical energy into electrical energy. Because of these unique properties, there has been much interest in using DE for energy harvesting,[6,17] including environmental sources such as ocean waves, water currents[18] and wind,[19] as well as human motions through heal strikes,[20] and knee bending.[21,22]

For small strains, a linear representation of the stress strain behavior is generally sufficient to model dielectric elastomers.[1] However, as the functionalities of DE are expanded, this nearly incompressible material experiences large deformations, requiring the use of nonlinear hyperelastic models to describe the behavior of materials ranging from synthetic polymers to biological tissues.[23,24] Examples of some prominent models include neo-Hookean, Mooney–Rivlin, Yeoh, and Ogden.[23–28] Although these models are useful in describing the mechanical behavior of the polymer used in the DE device, they have not been demonstrated to be sufficient to describe the electromechanical behavior of a DE device for two reasons. Firstly, these classical models do not address the constraint effects that compliant electrodes impose on the polymer substrate and, therefore, are unable to fully describe the mechanical behavior of the composite structure of the DE device. Secondly, electrical proprieties of the DE device, such as capacitance, are highly sensitive to the polymer thickness and surface area, which are directly related to the transverse and lateral strains for materials under uniaxial load, therefore requiring accurate modeling of the stretch ratios. A model capable of including these electrode-imposed constraints is crucial for accurate evaluation of the Maxwell stress and energy harvesting capacity of a DE device. To date, modeling of these constraints has never been examined.

The purpose of this paper is to develop and experimentally validate a novel approach to modeling the constraint effects of the compliant electrodes on the hyperelastic behavior, particularly the lateral contraction, of dielectric elastomers under uniaxial tension. To achieve this, an empirical *boundary coefficient* is introduced in the principal stretch ratio relations to account for the constraint effects. In the upcoming section, modifications to the basic hyperelastic constitutive equations which incorporate modeling of the boundary coefficient for uncharged DE are discussed. An experimental procedure to determine the boundary coefficient, based only on measureable variables, is proposed and tested on several DE devices in a later section. A model of the nonlinear stress–strain relations describing the hyperelastic behavior of DE undergoing uniaxial tension is derived next and, subsequently, this technique is extended to model the electromechanical coupling behavior of the DE. This modeling approach represents an improvement over current models as it provides a means to quantify the constraint effects of different electrodes on the dielectric polymer substrates undergoing uniaxial tension. It is demonstrated that this model provides a more accurate evaluation of the Maxwell stress developed in a composite electrode/dielectric polymer structure. Using the improved hyperelastic models, predicted values of the Maxwell stress are compared with experimental results.

Modeling of constraint effects of compliant electrodes

Basic equations of hyperelastic models

The basic hyperelastic model is first applied to an uncharged dielectric elastomer, which is assumed to be an isotropic, homogeneous, and incompressible hyperelastic material with negligible time-varying effects. The Cauchy principal stresses are determined from the derivative of the strain energy potential, W, with respect to the principal stretch ratios $\lambda_i = x_i/x_{i0}$[27,28]

$$\sigma_i = \lambda_i \frac{\partial W}{\partial \lambda_i} - p \quad \text{(no sum over the index)} \qquad i = 1, 2, 3 \tag{1}$$

where p is the volumetric hydrostatic pressure without shear. (Refer to Figure 1 for definition of the coordinates.) These parameters depend on the given geometric boundary conditions of the dielectric elastomer. The hydrostatic pressure, p, describes how the boundary conditions affect the internal pressure of a material undergoing deformation. This term must be found for a specific energy potential and device configuration. For instance, for an uncharged DE device in uniaxial tension experiencing no constraint in the transverse (x_3) direction, p is found by substituting the specific energy potential into the stress formula and then solving the equation $\sigma_3 = 0$. Using this process, the hydrostatic pressure is then back substituted into the stress formula, resulting in a set of nonlinear stress–strain relations. For example, the relations derived using the Yeoh energy potential model, $W_{Yeoh} = \sum_{i=1}^{3} c_i (I_1 - 3)^i$, can be shown to be[28]

$$\sigma_i = 2\left(\lambda_i^2 - \lambda_3^2\right)\left(C_1 + 2C_2(I_1 - 3) + 3C_3(I_1 - 3)^2\right), \qquad i = 1, 2, 3 \tag{2}$$

where the coefficients C_j depend on the material properties and $I_1 = \sum_{i=1}^{3} \lambda_i^2$ is the first invariant of the strain tensor.[29]

Characterization of compliant electrode induced edge boundary conditions

Consider a dielectric elastomer device under uniaxial tension in Figure 1, where σ_1 is the axial stress and σ_M represents the Maxwell stress induced by an electric field in the transverse (x_3) direction. Here, the effects of the constraints that compliant electrodes impose on the mechanical behavior of an uncharged dielectric

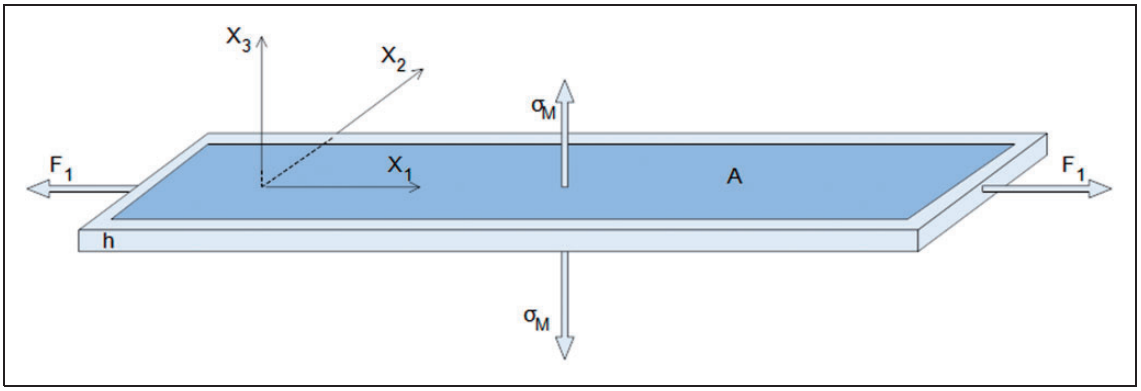

Figure 1. A dielectric elastomer device under uniaxial tension.

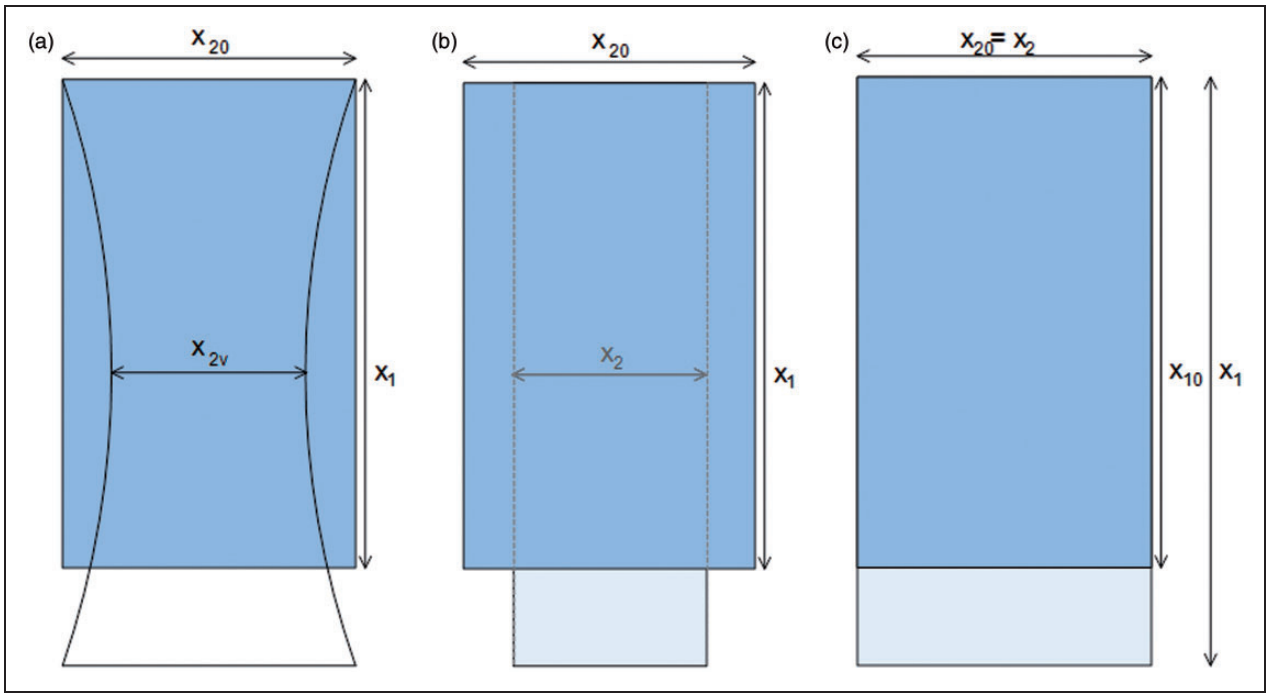

Figure 2. Possible modeling of boundary constraint conditions for strain in the x_2 direction. Bold lines denote constrained edges: (a) actual response; (b) unconstrained width; (c) constrained width.

polymer under uniaxial stretching are modeled first. The more general problem of the constraint effects on the electromechanical behavior of the DE will be examined in section "Electrostatic Maxwell stress".

The incompressibility of dielectric elastomer materials requires that its total volume remain the same regardless of the strains developed. For a thin film DE device under uniaxial tension, response in the lateral (x_2) direction depends on the edge boundary conditions of the film. When the ends in the x_1 direction are fixed and there is no external constraint on the material in the x_2 direction, the edges experience a contraction or narrowing at the center of the film, producing a concave curve as shown in Figure 2(a). It should be noted that, while this behavior occurs irrespective of the presence of the electrodes, the additional constraint effects from the electrodes vary depending on the electrode properties and have not been modeled previously.

Figure 2 compares the actual response of the material with two idealized limiting cases: zero stress (b) or zero strain (c) in the x_2 direction; these are the simple tension and pure shear cases, respectively, discussed by Ogden.[27] Simplified hyperelastic models respond to the lateral contraction effect by employing one of the two limiting boundary conditions, and thus fail to address the additional constraints that electrodes impose on the DE material. One of the primary purposes of this work is to establish a means to account for this behavior in composite thin film DE materials undergoing uniaxial stress. Throughout this study, the following terminology will be applied to the limiting cases for the specific condition of a composite film DE undergoing uniaxial tension. The zero lateral

stress, known as the *unconstrained boundary condition*, (Figure 2(b)) assumes that $\sigma_2 = 0$ for the polymer. Such an assumption is closest to the application where the electrode material is very compliant, as in the case of graphene powder dusted over the surface of the polymer. With this assumption, the strain in the x_2 direction is modeled as uniform along the entire edge of the polymer film, with the following stretch ratio relations[23]

$$\lambda_1 = \lambda, \lambda_2 = \frac{1}{\sqrt{\lambda}}, \lambda_3 = \frac{1}{\sqrt{\lambda}}$$
(unconstrained or simple shear) (3)

which indicate that stretching an unconstrained material results in a proportional reduction in both the thickness and the width of the material. Note that the above relations are expressed in terms of a single variable λ, the stretch ratio in the x_1 direction under a uniaxial stretch. The alternate limiting case, referred to here as the *fully constrained boundary condition* (Figure 2(c)), is more appropriate for some compliant electrode materials. For the fully constrained condition, the strain in the x_2 direction is assumed to be very small, and therefore $\lambda_2 = 1$. This model implies that only the thickness of the film changes directly as a result of the axial strain.

$$\lambda_1 = \lambda, \lambda_2 = 1, \lambda_3 = \frac{1}{\lambda}$$
(fully constrained or pure shear) (4)

It should be noted that, since $\lambda > 1$, uniaxial stretch of a fully constrained DE material results in a thinner dielectric material than the unconstrained case. This case is applicable when either the aspect ratio is very large (i.e. $x_1 \gg x_2$) or the edges of the film are constrained to provide the stress necessary to prevent the contraction.[25,30]

Kinematic modeling of the geometric constraints in a composite polymer/electrode

The mechanical behavior of a hyperelastic polymer is characterized by its stretch ratios λ_i which are required to satisfy both the incompressibility assumption ($\lambda_1\lambda_2\lambda_3 = 1$) and the constraints imposed on them by the boundary conditions. The relationships between the stretch ratios take different forms depending on the imposed edge boundary conditions, varying between the two limiting cases discussed above.

Partial constraint of the width (Figure 2(a)) can either be externally imposed, such as through the use of elastic constraints along the edge of the width of the film specifically designed to prevent pull in Brochu et al.,[25] or internally imposed through the structure of the film or electrodes. An example of an internally imposed constraint is the commercially available PolyPower DE film manufactured by Danfoss.[16,25] This DE material uses a silicon dielectric and a metalized electrode. The polymer has a special corrugated shape in the x_1 direction, allowing stretch only in that direction, while keeping its approximate width in the x_2 direction. This behavior allows for the use of highly conductive, but rigid metals for the electrodes. Through experimental observation described in section "Experimental procedure and determination of the boundary coefficient" of the PolyPower film as it is being stretched, it is can be observed that although the width is constrained, it still experiences a slight lateral contraction in the x_2 direction.

To model the lateral contraction of the elastomer, including the additional constraint effects from the compliant electrodes, we introduce a *boundary coefficient*, $0 \leqslant \kappa \leqslant 1$, which is constructed to describe the influence of the particular boundary constraint in the x_2 direction, with $\kappa = 0$ corresponding to the uniaxial unconstrained (Figure 2(b)) and $\kappa = 1$ corresponding to the uniaxial fully constrained width (Figure 2(c)) cases. From equations (3) and (4), employing a linear interpolation between the λ_2 of the two limiting boundary conditions, an "average" stretch ratio in terms of κ is defined

$$\lambda_{2avg} = \frac{x_{2avg}}{x_{20}} = \sqrt{\frac{1-(1-\lambda)\kappa}{\lambda}} \quad (5)$$

relating an average width, x_{2avg}, to λ and κ. This average width is defined such that the surface area $x_1 x_{2avg}$ is equivalent to the actual surface area as a result of the contraction (see Figure 3).

To determine λ_{2avg}, each side of the curvature is approximated as a parabola shown in Figure 3. In addition to being a reasonable mathematical approximation (second order approximation), we chose a parabola as the edge shape function based on observations of the actual devices under strain and the need for a function which can be readily described in terms of *measureable variables*: x_1, the stretched length, and x_{2v}, the width at the vertex of the parabola (the location where the dielectric elastomer width is minimum). Calculating the surface area of the stretched DE based on the parabola curve assumption and equating this area to $x_1 x_{2avg}$ give the average width and stretch ratio

$$\lambda_{2avg} = \frac{x_{2avg}}{x_{20}} = \frac{1}{3}\left(1 + 2\frac{x_{2v}}{x_{20}}\right) \quad (6)$$

It is important to note that although the actual response of the film is dependent on the immeasurable Maxwell stress, the above expression has been developed such that it is expressed entirely in terms of the original width and the stretched vertex width, two variables that can be directly visually measured.

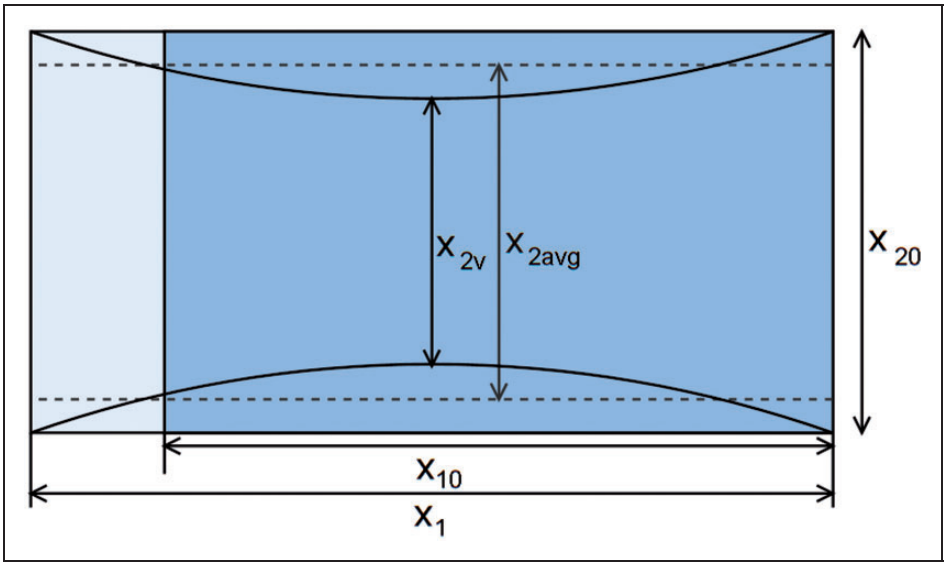

Figure 3. Illustration of the average width, x_{2avg}, with the actual condition.

Equating equations (5) and (6) leads to a compact formula for the boundary coefficient

$$\kappa = \frac{1}{\lambda - 1}\left(\lambda\left(\frac{x_{20} + 2x_{2v}}{3x_{20}}\right)^2 - 1\right) \tag{7}$$

Equations (5) and (7) provide a means to understand the relationship between the actual physical behavior of a thin film DE device undergoing uniaxial strain and the mathematical model based on idealized boundary conditions. The significance of equation (7) is that it allows for direct determination of κ based only on experimentally measureable geometric parameters: x_{20}, x_{2v}, and λ. Using this approach and the incompressibility condition, the stretch ratios, defined in terms of λ and κ, are

$$\lambda_1 = \lambda, \quad \lambda_2 = \sqrt{\frac{1 - (1 - \lambda)\kappa}{\lambda}}, \quad \lambda_3 = \frac{1}{\sqrt{\lambda(1 - (1 - \lambda)\kappa)}} \tag{8}$$

For uniaxial DE materials experiencing partial constraint of the width (such as the PolyPower), this formulation allows for a more accurate modeling of the actual constraint condition. The relationships (8) can be employed to model the entire range of boundary conditions between the unconstrained and fully constrained conditions, based on experimentally determined values of κ, and will be used in subsequent hyperelastic modeling of the stress–strain relations.

Experimental procedure and determination of the boundary coefficient

For a dielectric elastomer undergoing mechanical strain in the x_1 direction, the material deforms into a nonlinear curve in the x_2 direction (Figure 2(a)). The extent of this effect depends on the boundary constraint condition, where a nonconstraining electrode material such as graphene will produce a more pronounced nonlinear curve than a more rigid electrode material such as metal plating. In order to quantify the effects that compliant electrodes have on the lateral contraction effect described earlier, a mechanical test stand was developed to record the geometry of the film as a function of the stretch ratio λ.

The mechanical portion of the test stand is comprised of an instrumented linear motor with a built-in linear potentiometer and a force gage. The linear motor is computer controlled via a National Instruments data acquisition card (NI USB 6210) using a custom LabVIEW program. The DIGIT linear motor by Ultra Motion LLC comprised an 8 inch (203.2 mm) stroke lead screw linear shaft driven by a NEMA 17 stepper motor, and contains a potentiometer feedback used for both the position control of the motor and extension measurements. The motor is driven using the ST5-S driver, modulated through the analog input channel.

Force measurements were made using a full-bridge thin beam load cell from Omega. A fixture (Figure 4 lower insert) was utilized to house the strain gage load cells which constrained the measuring beam to an S bend deformation. This fixture was designed to be used either with one side fixed, or inline between two links. For this test stand, the fixed positioning method was used. The fixture shown in Figure 4 upper insert was used to restrain the elastomer DE film during the tests. It was designed to hold the DE polymer without slipping, while also assuring that a constant electrical connection was maintained between the electrodes and the output wires without rupturing the film. The fixture used was made of three layers of 1/4 inch polycarbonate plates, and is illustrated in the top insert in

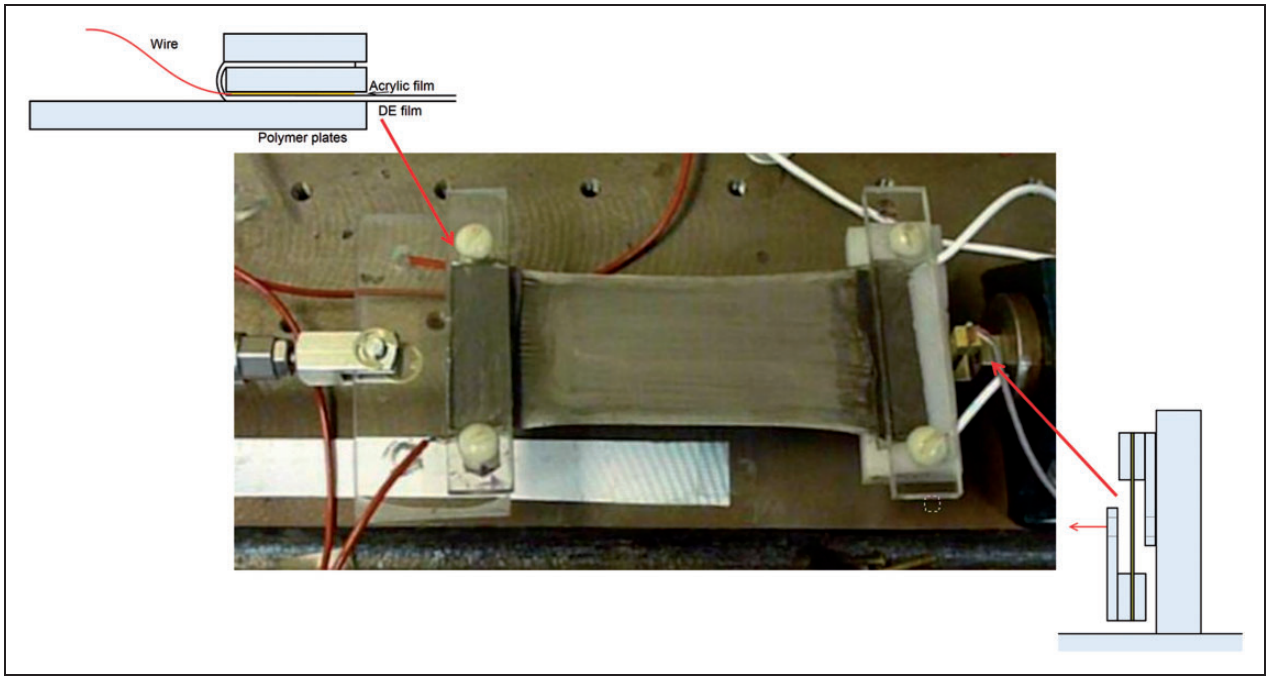

Figure 4. Lateral contraction of a silicone elastomer with graphene electrodes stretched by 27%. Inserts show the cross section of the fixture for the DE film and the S-bend strain gage force transducer setup.

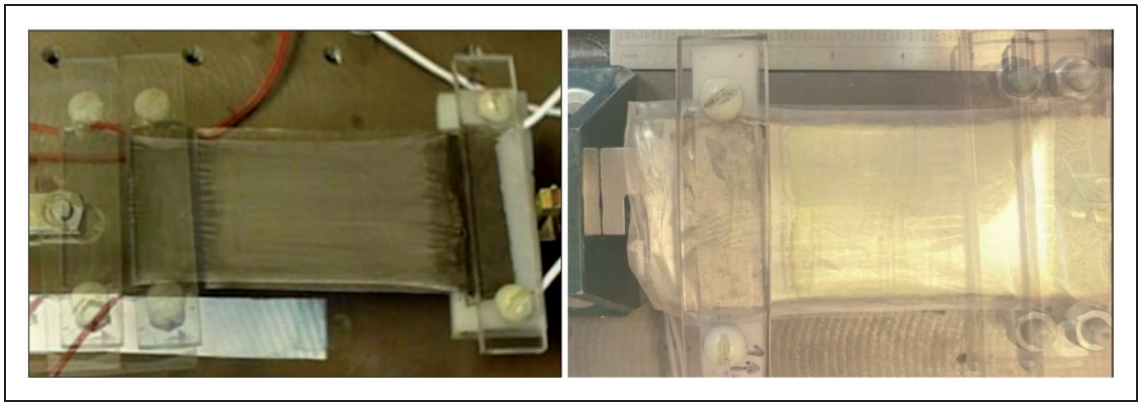

Figure 5. Superimposed images of unstretched ($\lambda = 1$) and stretched ($\lambda = 1.27$) DE film (left: graphene, right: PolyPower) demonstrates the lateral contraction of the film. greater contraction can be observed for graphene than for PolyPower.

Figure 4. The DE film was wrapped and sandwiched between the polycarbonate plates and clamped in place using non-conducting nylon screws. In addition to the DE film, on the bottom layer, the electrical wire contacted the electrode material on only one of the sides of the film, with an additional acrylic film to hold it in place to prevent pinching of the DE material. The fixture on the opposite side of the film is similar, except that the wire and acrylic contact the opposite electrode of the DE film.

Figure 4 provides a visual representation of the lateral contraction exhibited when a silicone elastomer with graphene electrodes is strained to a stretch ratio of $\lambda = 1.27$, which was determined by comparison of the linear motor potentiometer readings in the unstretched and stretched positions. Experimental procedure for measurements of the geometric variables required to determine κ was performed as follows. Images of the material in the unstretched position and the stretched position were captured for a given stretch ratio, and the two images were superimposed upon one another (see Figure 5). An onscreen digital measurement tool (Screen RULER developed by Delphi Programming) was then used to measure the width for each condition. The resolution of the onscreen measurement tool, which depended on the resolution of the images captured, was determined to be at most ± 0.077 mm for each of the conditions included.

Utilizing these measurements, the value of κ was determined for a given configuration using equation (7). To assure that the dielectric polymer behaved similarly with each electrode material, the

Table 1. Boundary coefficient κ and average width stretch ratio λ_{2avg} for DE films.

Electrode material	Axial stretch ratio (λ)	κ	λ_{2avg}	Comparison of λ_{2avg} with limiting cases (% difference)	
				$\kappa = 0$ case	$\kappa = 1$ case
Graphene	1.28	0.23	0.91	−3.1	9.7
Carbon grease	1.13	0.31	0.96	−1.9	4.1
	1.09	0.64	0.98	−2.8	1.5
PolyPower	1.18	0.63	0.97	−5.2	3.0
	1.28	0.64	0.96	−8.0	4.2

unmetalized dielectric film from the PolyPower material was used to provide the dielectric polymer substrate for each device (thickness $x_{30} = 80\ \mu$m, dielectric permittivity $\varepsilon = 3.1$[25]). Three sets of materials (graphene on PolyPower polymer, carbon grease on PolyPower polymer, and PolyPower itself) were tested, and their values of κ were found and tabulated in Table 1. It is noted that the values of κ depend strongly on the electrode material, but are fairly constant throughout the experimental range for PolyPower. These results thus imply that κ is likely independent of the stretch ratio but depends only on the material properties. Moreover, with the electrodes providing more internal constraints within the PolyPower, this DE behaves closer to the fully constrained case ($\kappa = 1$). In Table 1, the lateral stretch ratio, λ_{2avg}, estimated using the empirical κ value, is compared with the lateral stretch ratio calculated for both limiting cases, $\lambda_{2[\kappa=0]} = 1/\sqrt{\lambda}$ and $\lambda_{2[\kappa=1]} = 1$. This comparison is provided for three different electrode materials with distinctly different boundary condition coefficients. In addition, there is included a comparison of three different axial stretch ratios for the PolyPower sample.

It can be seen that the deficiencies of the classical limiting models become more pronounced as the constraint condition deviates from the given limiting cases. Departure from the classical models also grows with increasing λ. The development of this boundary coefficient for the uniaxial DE is significant as it provides a means to model the lateral constraint condition, in order to more accurately describe the stress–strain relation and electromechanical behavior of a uniaxial DE device. Following these derivations, the boundary coefficient concept is extended in section "Electrostatic Maxwell stress" to develop general expressions for the mechanical response in the axial direction induced by the Maxwell stress in order to characterize the electromechanical behavior of a uniaxial charged DE.

Hyperelastic stress–strain relation incorporating kappa

Incorporating the boundary coefficient κ into the principal stretch ratios (8) provides a hyperelastic stress–strain model for the dielectric elastomer coupled with compliant electrodes under uniaxial loading. For example, from equation (2), the general stress–strain relations for the modified Yeoh model (superscripted IY below) can be shown to become

$$\begin{aligned}
\sigma_1^{MY} &= 2\left(\lambda^2 - \frac{1}{\lambda(1-(1-\lambda)\kappa)}\right) \\
&\quad \times \left(\begin{array}{l} C_1 + 2C_2\left[\begin{array}{l}\lambda^2 + \dfrac{1}{\lambda(1-(1-\lambda)\kappa)} \\ +\dfrac{(1-(1-\lambda)\kappa)}{\lambda} - 3\end{array}\right] \\ +3C_3\left[\begin{array}{l}\lambda^2 + \dfrac{1}{\lambda(1-(1-\lambda)\kappa)} \\ +\dfrac{(1-(1-\lambda)\kappa)}{\lambda} - 3\end{array}\right]^2 \end{array} \right) \\
\sigma_2^{MY} &= 2\left(\lambda(1-(1-\lambda)\kappa) - \frac{1}{\lambda(1-(1-\lambda)\kappa)}\right) \\
&\quad \times \left(\begin{array}{l} C_1 + 2C_2\left[\begin{array}{l}\lambda^2 + \dfrac{1}{\lambda(1-(1-\lambda)\kappa)} \\ +\dfrac{(1-(1-\lambda)\kappa)}{\lambda} - 3\end{array}\right] \\ +3C_3\left[\begin{array}{l}\lambda^2 + \dfrac{1}{\lambda(1-(1-\lambda)\kappa)} \\ +\dfrac{(1-(1-\lambda)\kappa)}{\lambda} - 3\end{array}\right]^2 \end{array} \right)
\end{aligned} \tag{9}$$

where $\sigma_3^{MY} = 0$ is imposed to solve for the hydrostatic pressure term p. This set of equations provides a general formula relating the axial stretch ratio λ of the thin film to the generated stresses in each of the three directions. The coefficients C_j for each of these models can be found through experimental measurements, and in many cases they are available in the Wissler and Mazza.[28] In our tests, the coefficients C_j were determined by curve fitting experimental data to a model equation (e.g. equation (9) for the improved Yeoh model) for each material and geometry investigated while undergoing uniaxial strain. Force versus stretch ratios in uniaxial tensile tests were obtained for the three sets of DE films found in Table 1 and curved fitted to the three improved models of neo-Hookean, Mooney–Rivlin, and Yeoh with κ incorporated. It was found that the r^2 values ("goodness of fit", with

$r^2 = 1$ for a perfect fit) of the improved Yeoh model were closest to 1 (about 0.998) for uniaxial tests up to 50% elongation. Although the hyperelastic dielectric is capable of undergoing much larger elongations, for the dielectric elastomer application, elongation up to only 50% was considered because beyond this strain, the compliant electrodes experience large degradation of their electrical performance. Based on these results, the Yeoh model was thus chosen to estimate the Maxwell stress in section "Electrostatic Maxwell stress". Comparison of the coefficients for each of the conditions demonstrated that there was a large variation based on the compliant material which was incorporated into the composite film, indicating that there proper modeling of the effect of the constraint condition is necessary for accurate modeling.

The general form of the improved Yeoh stress–strain model in equation (9) is quite cumbersome to examine analytically. In an attempt to simplify the analytical expressions, we first investigated the sensitivity of equation (9) to the constraint conditions to determine to what extent variation in κ affects the coefficients C_j of the stress–strain curve generated using the improved Yeoh model from empirical data. By comparing curves generated from the same data for several values of κ, it was determined that the model coefficients were not greatly affected by the value of κ. However, it was found that the stress in the x_2 direction was very sensitive to κ. This suggests that both the width and the thickness are influenced by the constraints imposed by the electrode material. Based on these results, the boundary coefficient κ must be included when modeling geometry sensitive variables such as the capacitance and the Maxwell stress for a dielectric elastomer. However, for the stress–strain relationship in the x_1 direction, hyperelastic models based on either of the two limiting cases (either $\kappa = 0$ or $\kappa = 1$) can be used as they greatly simplify the calculations without much loss of accuracy.

Electrostatic Maxwell stress

The Maxwell stress, also termed electrostatic stress, is caused by the force of opposite charges attracting one another from opposite parallel plates. An electrostrictive stress is also associated with a parallel plate dielectric placed within an electric field; however, for the dielectric polymers investigated, the electrostrictive coefficient is assumed to be much smaller than the electrostatic, and is thus neglected.[14] The electromechanical coupling of the dielectric elastomer is therefore modeled based on the Maxwell stress alone.

The Maxwell stress developed by an electric field, E, is directly related by the permittivity of the dielectric, ε, and can be written in terms of a bias voltage and the dielectric thickness

$$\sigma_M = -\varepsilon E^2 = -\varepsilon\left(\frac{V}{x_3}\right)^2 \tag{10}$$

Since the Maxwell stress acts only in the direction perpendicular to the electrode surface area and this is the only stress experienced in that direction, invoking the relation $V = \frac{x_3}{\varepsilon x_1 x_2} Q$, for a given charge, one can write the Maxwell stress as[21]

$$\sigma_{3M} = \sigma_M = -\frac{1}{\varepsilon}\left(\frac{Q}{x_1 x_2}\right)^2 \tag{11}$$

To evaluate the Maxwell stress, a similar methodology is employed as was previously used in the mechanical strain case to first determine the hydrostatic pressure. To differentiate the stretch ratio due to the Maxwell stress from that due to the mechanical strain, new stretch ratios, termed Maxwell stretch ratios, $\tilde{\lambda}_i$, are defined to describe the change in the displacement field of the film as a result of the Maxwell stress generated due to a charge across the DE film (which acts as a capacitor), independent of any mechanical stretch. In the following two sections, we first examine the effect of the Maxwell stress purely due to an electric field with no mechanical loading (i.e. $\lambda = 1$). This analysis is then expanded in section "Electromechanical stresses due to combined stretch and charge" to include strains due to mechanical stresses, where $\lambda > 1$. In establishing the relationships of the Maxwell stretch ratios, $\tilde{\lambda}_i$, in terms of κ, the following assumptions about the electromechanical behavior of the material are imposed:

- The test setup utilizes a position control in the axial direction to isolate the axial force induced by the Maxwell stress. Hence, the position in the x_1 direction is fixed and there can be no additional stretch due to the Maxwell stress, i.e., $\tilde{\lambda}_1 = 1$.
- σ_3 is assumed to be equal to the Maxwell stress, thus allowing σ_M to be incorporated into the stress formula, $\sigma_{3M} = \tilde{\lambda}_3\left(\partial W/\partial\tilde{\lambda}_3\right) - p = \sigma_M$.

Electrostatic pressure and stresses for the limiting cases

Limiting case of uniaxial strain: Constrained lateral edges (pure shear). To model the Maxwell stretch ratios, the limiting cases shown in Figure 2(b) and (c) were considered first. The fully constrained condition provides the most direct relationship between σ_M and the stress in the x_1 direction. In this case, the DE film is constrained in both x_1 and x_2 directions, and hence there is no stretch in either direction. Assuming that the Maxwell stress is evenly distributed across the surface of the film, and imposing the incompressibility of the hyperelastic polymer, this configuration results in a situation similar to a rigid box, in which stresses are generated in all directions, as a result of the Maxwell stress, σ_M, in the x_3 direction as demonstrated in Figure 6.

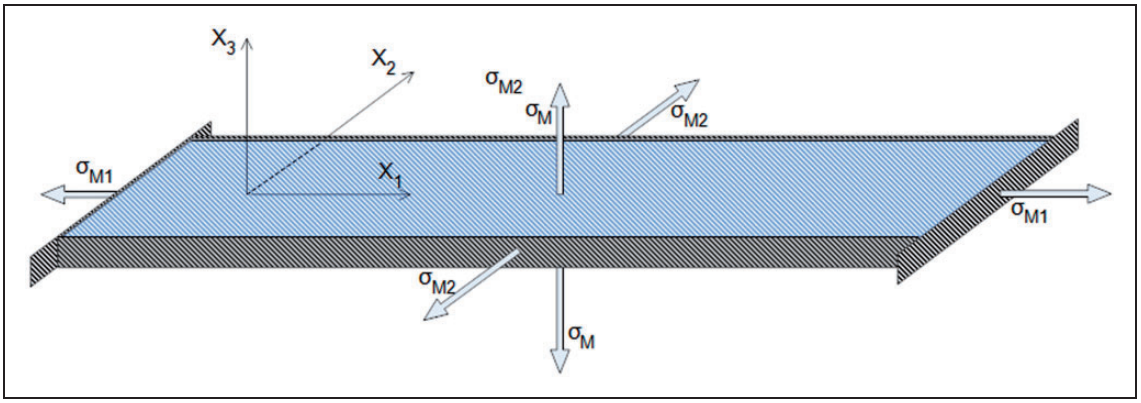

Figure 6. Conceptualization of the stress field in a DE film enclosed by rigid constraints (idealized fully constrained width condition).

Incorporating this idealized condition into the model results in the following Maxwell stretch ratios

$$\tilde{\lambda}_1 = 1, \quad \tilde{\lambda}_2 = 1, \quad \tilde{\lambda}_3 = 1$$
(fully constrained limiting case) (12)

This implies a perfect transmission of the Maxwell stress to each edge of the film, indicating that the stress in the measurement direction (x_1) is equivalent to the Maxwell stress generated by the capacitor.[31] Therefore, for the situation where there is no mechanical strain, the dimensions remain constant, and the stress in the x_1 direction resulting from the Maxwell stress simplifies to

$$\sigma_{1M} = \sigma_{3M} = \sigma_M = -\varepsilon\left(\frac{V}{x_{30}}\right)^2 = -\frac{1}{\varepsilon}\left(\frac{Q}{x_{10}x_{20}}\right)^2$$
(fully constrained limiting case) (13)

Limiting case of uniaxial strain: Unconstrained lateral edges (simple tension). The unconstrained boundary condition presents a slightly more complex situation, since the stretch ratio in the x_2 direction is unknown, as illustrated in Figure 7. However, since there is no stress generated in the x_2 direction in this limiting case, $\sigma_2 = 0$ and, therefore, it is still possible to determine the stress in the x_1 direction. Recalling that the DE is fixed in the x_1 direction, the Maxwell stretch ratios thus become

$$\tilde{\lambda}_1 = 1, \quad \tilde{\lambda}_2 = \tilde{\lambda}, \quad \tilde{\lambda}_3 = \frac{1}{\tilde{\lambda}}$$
(unconstrained limiting case) (14)

Employing the Yeoh hyperelastic model, the stress equations become

$$\sigma_{iM} = \tilde{\lambda}_i\frac{\partial W}{\partial \tilde{\lambda}_i} - p = 2C_1\tilde{\lambda}_i + 4C_2\tilde{\lambda}_1\left(\tilde{I}_1 - 3\right) + 6C_3\tilde{\lambda}_i\left(\tilde{I}_1 - 3\right)^2 - p \quad \text{(no sum over the index)}$$
(15)

where $\tilde{I}_1 = \sum_{i=1}^{3}\tilde{\lambda}_i^2$, with $\tilde{\lambda}_i$ given by (14), and $\sigma_{2M} = 0$, $\sigma_{3M} = \sigma_M$.

To determine σ_1, both the hydrostatic pressure p and the stretch ratio, $\tilde{\lambda}$, must be found. The hydrostatic pressure can be found as a function of $\tilde{\lambda}$ and σ_M by using the stress equation (15) in the x_3 direction. The result is then substituted into equation (15) to yield

$$\sigma_{1M} = 2\left(1 - \frac{1}{\tilde{\lambda}}\right)\left[C_1 + 2C_2\left(1 + \tilde{\lambda}^2 + \frac{1}{\tilde{\lambda}^2} - 3\right) + 3C_3\left(1 + \tilde{\lambda}^2 + \frac{1}{\tilde{\lambda}^2} - 3\right)^2\right] + \sigma_M$$
$$\sigma_{2M} = 2\left(\tilde{\lambda} - \frac{1}{\tilde{\lambda}}\right)\left[C_1 + 2C_2\left(1 + \tilde{\lambda}^2 + \frac{1}{\tilde{\lambda}^2} - 3\right) + 3C_3\left(1 + \tilde{\lambda}^2 + \frac{1}{\tilde{\lambda}^2} - 3\right)^2\right] + \sigma_M = 0$$
$$\sigma_{3M} = \sigma_M$$
(16a–c)

At this point, it is possible to determine the Maxwell stretch ratio, $\tilde{\lambda}$, by using equation (16b) as follows. The value of $\tilde{\lambda}$, which results from a constant Maxwell stress, is named the *equilibrium stretch ratio* because it describes the stretch of the material as it is experiencing a constant charge. In order to find $\tilde{\lambda}$, equation (16c) is rewritten in terms of $\tilde{\lambda}$ using equations (11) and (14)

$$\sigma_{3M} = \sigma_M = -\frac{1}{\varepsilon}\left(\frac{Q}{x_{10}x_{20}\tilde{\lambda}_1\tilde{\lambda}_2}\right)^2 = -\frac{1}{\varepsilon}\left(\frac{Q}{x_{10}x_{20}}\right)^2\frac{1}{\tilde{\lambda}^2}$$
(17)

The above result is then back substituted into equation (16b), and numerical root finding is utilized to determine the equilibrium stretch ratio for the given conditions. The result for this stretch ratio is used to obtain the effective stress in the x_1 direction due to the Maxwell stress, σ_{1M}, by equation (16a).

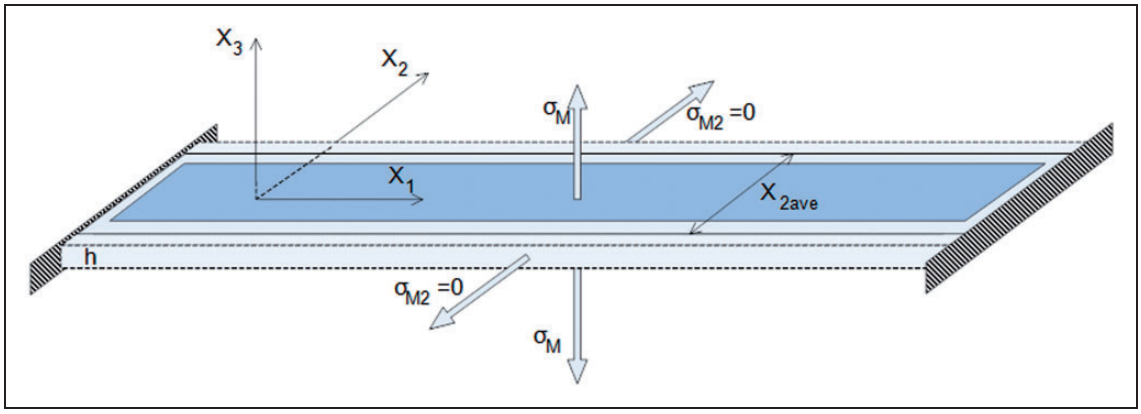

Figure 7. Conceptualization of the stress field in a DE film with no constraint in x_2 direction (idealized unconstrained width condition).

Electrostatic pressure and stresses for the general uniaxial DE

The stretch ratios associated with this condition can be described using the boundary coefficient, κ, defined in section "Modeling of constraint effects of compliant electrodes". Since the position in the x_1 direction is fixed, the Maxwell stretch ratios are defined as the linear interpolation between the two limiting cases

$$\tilde{\lambda}_1 = 1,\ \tilde{\lambda}_2 = \tilde{\lambda} + (1-\tilde{\lambda})\kappa,\ \tilde{\lambda}_3 = \frac{1}{\tilde{\lambda} + (1-\tilde{\lambda})\kappa} \quad (18)$$

which can be compared with the mechanical stretch ratios defined in equation (8). Using these Maxwell stretch ratio definitions, the stress generated in the x_1 direction can be defined as a function of κ by considering the stress in the x_2 direction. When the width of the DE film is partially constrained, σ_2 is no longer zero, therefore, it contributes to the transmission of the stress in the $x_1$direction. With the width not fully constrained, the stretch ratio $\tilde{\lambda}$ is unknown, resulting in an underdetermined system

$$\begin{aligned}\sigma_{1M} &= 2\tilde{\Gamma} - p \\ \sigma_{2M} &= 2\left(\tilde{\lambda} + (1-\tilde{\lambda})\kappa\right)\tilde{\Gamma} - p \neq 0 \\ \sigma_{3M} &= 2\frac{1}{\tilde{\lambda} + (1-\tilde{\lambda})\kappa}\tilde{\Gamma} - p = \sigma_M \end{aligned} \quad (19a\text{–}c)$$

where, $\tilde{\Gamma} = C_1 + 2C_2(I_1 - 3) + 3C_3(I_1 - 3)^2$, $I_1 = \sum_{i=1}^{3} \tilde{\lambda}_i^2$ with $\tilde{\lambda}_i$ given by equation (18), and

$$\sigma_M = -\frac{1}{\varepsilon}\left(\frac{Q}{x_{10}x_{20}}\right)^2 \frac{1}{\left(\tilde{\lambda} + (1-\tilde{\lambda})\kappa\right)^2}.$$

If additional measurements are taken to determine the position, x_2, after the Maxwell stress is applied to a material of a known constraint condition, then the equilibrium stretch ratio, $\tilde{\lambda}$, can be found by comparing x_2 before and after charging. Based on this, it is possible to determine directly the stress in the x_1 direction due to the Maxwell stress using the stress equations above. In the absence of experimental data, we adopt an approach that involves linearly interpolating $\tilde{\lambda}$ based on the stretch ratios of the limiting cases, $\tilde{\lambda}_c$, $\tilde{\lambda}_u$ where $\tilde{\lambda}_c = 1$ and $\tilde{\lambda}_u$ is numerically found using the technique described previously for the unconstrained width case. Once the interpolated $\tilde{\lambda}$ is found, it is back-substituted into the stress equations, where p is determined from equation (19c), resulting in the following expression for the effective Maxwell stress in the x_1 direction

$$\sigma_{1M} = 2\left(1 - \frac{1}{\tilde{\lambda} + (1-\tilde{\lambda})\kappa}\right)\tilde{\Gamma} + \sigma_M \quad (20)$$

where $\tilde{\Gamma}$ and σ_M are defined above, after equation (19).

This formulation presents a means to estimate both the Maxwell stress, σ_M, and the stress generated in the axial direction as a result of the Maxwell stress, σ_{1M}, based solely on the DE configuration and the stretch ratio in the lateral direction, $\tilde{\lambda} = \tilde{\lambda}_2$, which can be determined through direct measurement of the DE film.

Electromechanical stresses due to combined stretch and charge

When a DE device is undergoing a uniaxial strain in the x_1 direction in addition to an electric charge, the total stress is determined based on the combined effects of both the mechanical stress and the Maxwell stress. For a general uniaxial thin film DE in tension experiencing constant electric charge, the Maxwell stress (11) is obtained based on the geometry resulting from the product of the stretch ratios

$$\sigma_M = -\frac{1}{\varepsilon}\left(\frac{Q}{x_{10}x_{20}}\frac{1}{\lambda_1\tilde{\lambda}_1\lambda_2\tilde{\lambda}_2}\right)^2 \quad (21)$$

where the stretch ratios are determined based on the constraint conditions of the device. For example, the electromechanically coupled Maxwell stress formulations for the limiting cases can be shown to be as follows.

Fully constrained condition. The fully constrained condition results in $\tilde{\lambda} = 0$, and $\sigma_{1M} = \sigma_{3M}$ resulting in

$$\sigma_{1M} = \sigma_{3M} = -\frac{1}{\varepsilon}\left(\frac{Q}{x_{10}x_{20}\lambda}\right)^2 = -\frac{1}{\varepsilon}\left(\frac{Q}{x_{10}x_{20}}\right)^2\frac{1}{\lambda^2} \quad (\text{fully constrained}) \tag{22}$$

Once the effective Maxwell stress is found, the total stress in the x_1 direction becomes the sum of the mechanical stress and the effective Maxwell stress.

Unconstrained condition. For the unconstrained case, $\lambda_1\tilde{\lambda}_1\lambda_2\tilde{\lambda}_2 = \lambda \times 1 \times \frac{1}{\sqrt{\lambda}} \times \tilde{\lambda} = \sqrt{\lambda}\tilde{\lambda}$, is utilized to determine the Maxwell stress in the x_3 direction

$$\sigma_M = -\frac{1}{\varepsilon}\left(\frac{Q}{x_{10}x_{20}\sqrt{\lambda}\tilde{\lambda}}\right)^2 = -\frac{1}{\varepsilon}\left(\frac{Q}{x_{10}x_{20}}\right)^2\frac{1}{\lambda\tilde{\lambda}^2} \quad (\text{unconstrained}) \tag{23}$$

This term now specifies the Maxwell stress perpendicular to the mechanical motion, and the equilibrium stretch ratio $\tilde{\lambda}$ due to the effect of the Maxwell stress must be found in order to determine the effective Maxwell stress in the x_1 direction. The procedure to find $\tilde{\lambda}$ was described previously, utilizing the condition $\sigma_{2M} = 0$ stated in equation (16b).

General uniaxial condition. When the product of the stretch ratios for the unconstrained condition are utilized for the general case, $\lambda_1\tilde{\lambda}_1\lambda_2\tilde{\lambda}_2 = \lambda \times 1 \times \sqrt{\frac{1+(\lambda-1)\kappa}{\lambda}} \times \left(\tilde{\lambda} + (1-\tilde{\lambda})\kappa\right)$, the Maxwell stress can be defined in the x_3 direction as

$$\sigma_M = -\frac{1}{\varepsilon}\left(\frac{Q}{x_{10}x_{20}}\right)^2 \frac{1}{\lambda(1+(\lambda-1)\kappa)\left(\tilde{\lambda} + (1-\tilde{\lambda})\kappa\right)^2} \tag{24}$$

This provides a comprehensive means for determining the Maxwell stress when the equilibrium stretch ratio due to Maxwell stress, $\tilde{\lambda}$, is known (either experimentally or by estimation). Using σ_M and $\tilde{\lambda}$, the effective Maxwell stress in the x_1 direction, σ_{1M}, can be estimated from (16a). Once the stresses due to both the mechanical strain and the electrical charge are known, the total stress in the x_1 direction is the sum of the mechanical stress based on the improved Yeoh model, σ_1^{IY} from (9), and the effective Maxwell stress, σ_{1M} from equation (20)

$$\sigma_1 = \sigma_1^{IY} + \sigma_{1M} \tag{25}$$

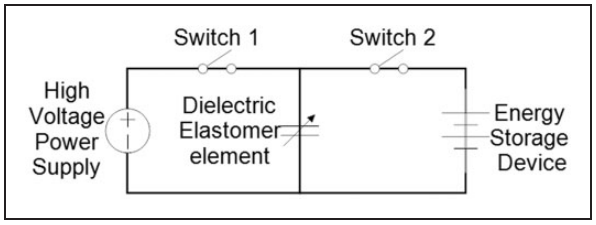

Figure 8. Schematic of circuit for charging/discharging a DE film.

Using this formulation, it is possible to estimate the axial stress generated in a thin film DE under uniaxial mechanical loading and electrical loading, based solely on the DE configuration and the loading conditions.

Experimental results

The experimental measurement of the force in the x_1 direction generated by the Maxwell stress was performed using the test stand described in section "Experimental procedure and determination of the boundary coefficient". In order to charge the DE device to the required voltage, a power supply system was developed to provide up to 3500 V of electricity to the DE device, and then discharge the device while measuring the power dissipated. In addition to the dielectric elastomer itself, this circuit was comprised of three computer regulated high power components: a high voltage power supply and two switches. A voltage divider was also included to provide a low voltage output, collected by the DAQ board. A schematic of the circuit used to supply the high voltage power and control the discharge is shown in Figure 8. The power supply charged the DE capacitor when the first switch was closed, and discharged the capacitor through the voltage divider when the second switch was closed. The resistances used for the voltage divider could be changed between the tests, and were selected based on the maximum voltage measured.

Using this test stand, the force in the x_1 direction, generated as a result of the Maxwell stress, was determined by measuring the force required to stretch the film to a specified stretch ratio when it was both uncharged and charged due to an electrical loading. A sample result is shown in Figure 9. As expected, the Maxwell stress generated across the surface in the x_3 direction results in a decrease in the force measured in the x_1 direction, reflecting the relaxing of the material in the x_1 and x_2 directions as the material is compressed in the x_3 direction.

Figure 10 compares the axial force induced by the Maxwell stress modeled using equation (19) with the experimentally measured values for each of the different materials investigated. In this figure, the error between the force in the x_1 direction estimated by the hyperelastic model using the measured κ values,

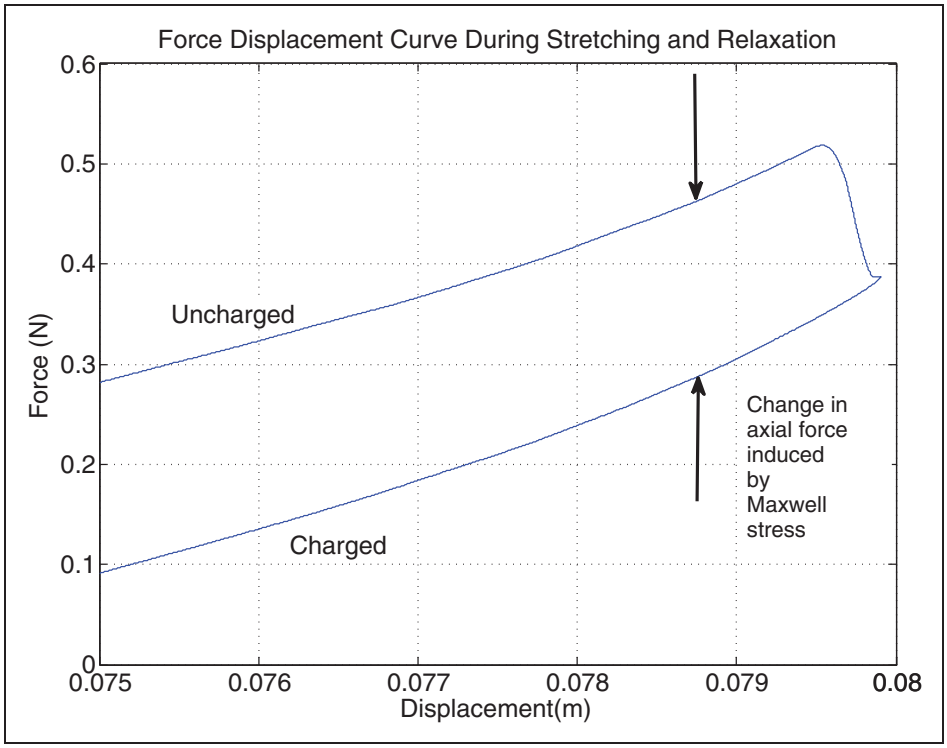

Figure 9. Illustration of the method used to measure the force induced on a uniaxial DE in the axial (x_1) direction due to Maxwell stress.

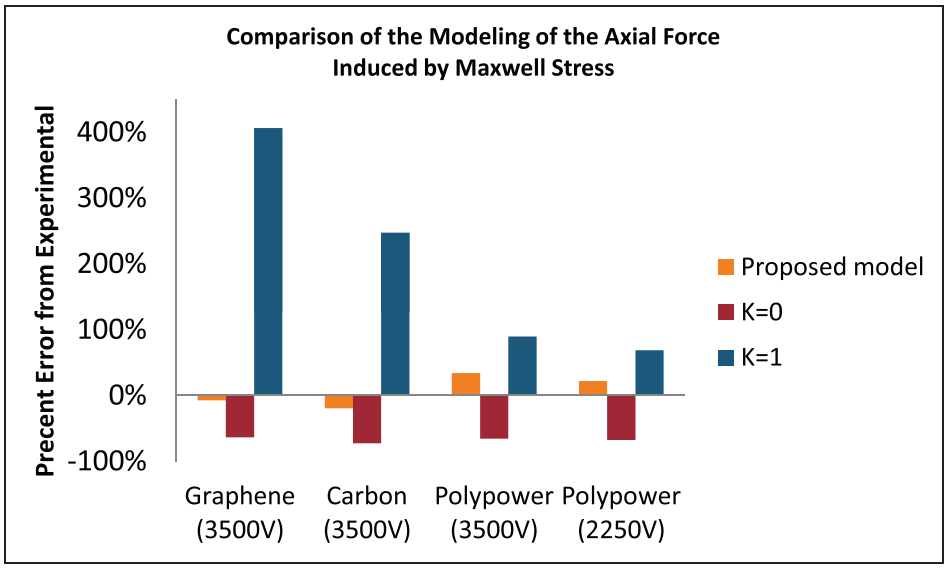

Figure 10. Comparison of the percent error between the measured axial force of DE under electrical loading and modeled axial force induced by the Maxwell stress for the proposed model using empirical values of K and the two limiting boundary conditions.

and the force measured in the x_1 direction when the DE film is electrically loaded is calculated as the difference between the modeled and experimental force divided by the experimental force. The percent error for the proposed model is shown along with the error in the force estimated using the limiting cases.

When the unconstrained boundary condition ($\kappa = 0$) is assumed, the axial force induced by the Maxwell stress is consistently underestimated. This result is predicted by equation (18), which implies that the modeled cross-sectional area of the DE is less while the modeled thickness is greater than the corresponding dimensions of the actual response. For the same reason, the fully constrained case ($\kappa = 1$), greatly overestimates the induced force, demonstrate the value of incorporating the boundary condition effects into the Maxwell stress model. The discrepancy between the modeled and measured axial induced force differs

for different compliant electrode materials, indicating once again that the mechanical properties of the compliant electrode play an important role in the mechanical behavior of the material, even when undergoing an electrically induced strain. While these results demonstrate the importance of modeling the constraint effects, it is important to note that they were made with a limited number of samples and in a very specific configuration. Additional measurements over a wide range of configurations are recommended in order to further expand the trend demonstrated here to a general DE film.

Conclusions

In this paper, an empirical boundary coefficient, κ, is introduced to model the constraint effects of the compliant electrodes on the lateral contraction of thin film, single layer dielectric elastomers undergoing uniaxial stretch. The boundary coefficient is defined based on an averaged stretch ratio concept and expressed in terms of geometric variables that can be measured experimentally. Experimental results show that κ is dependent only on the material properties and not on the stretch ratio. The development of this boundary coefficient to determine the response of the dielectric elastomer provides a means to incorporate the constraint conditions into the stress–strain relations for a given configuration. It is also shown that, while the boundary coefficient must be employed in the modeling of geometry sensitive variables such as capacitance and Maxwell stress, it has negligible effect on the calculation of the axial stress of the material under uniaxial stretching with no electrical load. Values of the boundary coefficient for several samples were obtained experimentally and, subsequently, used to derive an empirical hyperelastic model of the electromechanical behavior of the dielectric elastomer under coupled uniaxial tension and electrical load. Comparison of the experimental and predicted values of the axial force induced by the electrical loading based on the modified model shows favorable agreement, while simplified models without the constraint effects, substantially underestimate (when lateral edge of the material is assumed fully unconstrained) or overestimate (when assumed fully constrained) the Maxwell stress.

Although the modeling considered here is for uniaxial tension, the proposed approach lays a foundation for problems with more complex loading conditions. The empirical approach may also be adopted to examine similar geometric constraint effects in other composite structures in order to obtain specific stress–strain relations for those conditions as well.

Acknowledgements

The authors would like to gratefully acknowledge the Division of Research and the Graduate School of Wayne State University for their support of this work. The second author would also like to acknowledge support from the Signal Processing Key Laboratory of Zhejiang Province at Zhejiang University of Technology, Hangzhou, China.

Declaration of conflicting interests

The authors declared no potential conflicts of interest with respect to the research, authorship, and/or publication of this article.

Funding

The authors received no financial support for the research, authorship, and/or publication of this article.

References

1. Leo DJ. *Engineering analysis of smart material systems*. Blacksburg, VA: John Wiley and Sons, Inc, 2007.
2. Bar-Cohen Y. *Electroactive polymer (EAP) actuators as artificial muscles: Reality, potential, and challenges*. Cardiff: SPIE Press. 2004, p.816.
3. Bar-Cohen Y. Electroactive polymers as an enabling materials technology. *Proc IMechE, Part G: J Aerospace Engineering* 2007; 221: 553–564.
4. Biddiss E and Chau T. Electroactive polymeric sensors in hand prostheses: Bending response of an ionic polymer metal composite. *Med Eng Phys* 2006; 28: 568–578.
5. Paulo J and Gaspar PD. Review and future trend of energy harvesting methods for portable medical devices. In: *World congress on engineering 2010 WCE 2010,* 30 June to 2 July 2010. Hong Kong, China: IAENG International Association of Engineers, p. 6.
6. Chiba S, Waki M, Kornbluh R, et al. Innovative power generators for energy harvesting using electroactive polymer artificial muscles. In: TISfOE (ed.) *Electroactive polymer actuators and devices (EAPAD),* 10–13 March 2008. San Diego, CA: SPIE, pp.692715-1 (9 pp.).
7. Jean-Mistral C, Basrour S and Chaillout JJ. Comparison of electroactive polymers for energy scavenging applications. *Smart Mater Struct* 2010; 19: 085012 (14 pp.).
8. Pelrine R, Kornbluh R, Joseph J, et al. High-field deformation of elastomeric dielectrics for actuators. *Mater Sci Eng C: Biomimet Supramol Syst* 2000; C11: 89–100.
9. McKay T, O'Brien B, Calius E, et al. An integrated dielectric elastomer generator model. In: *Electroactive polymer actuators and devices (EAPAD)*, 8–11 March 2010. San Diego, CA: SPIE - The Society of Photo-Optical Instrumentation Engineers (SPIE); American Society of Mechanical Engineers.
10. Min K, Jung JY, Han TH, et al. Graphene electrodes for artificial muscles. *Mol Cryst Liq Crystals* 2011; 539: 260–265.
11. Kwon H-Y, Kuang Jun A, Junmo K, et al. Transparent active skin. In: *Electroactive polymer actuators and devices (EAPAD)*, 7–10 March 2011. San Diego, CA: SPIE - The International Society for Optical Engineering, p. 79760T (8 pp.).
12. Lau G-K, Goh SC-K and Shiau L-L. Dielectric elastomer unimorph using flexible electrodes of electrolessly deposited (ELD) silver. *Sens Actuat A* 2011; 169: 234–241.

13. Yuan W, Li H, Brochu P, et al. Fault-tolerant silicone dielectric elastomers. *Int J Smart Nano Mater* 2010; 1: 40–52.
14. Jean-Mistral C, Basrour S and Chaillout JJ. Modelling of dielectric polymers for energy scavenging applications. *Smart Mater Struct* 2010; 19: 105006 (11 pp.).
15. Benslimane M, Tryson MJ, Oubak J, et al. Scalable design of DEAP for energy harvesting utilizing PolyPower. *SPIE*, 2011, p. 79760I.
16. Iskandarani YH, Jones RW and Villumsen E. Modeling and experimental verification of a dielectric polymer energy scavenging cycle. In: *Electroactive polymer actuators and devices (EAPAD)*, 9 March 2009. San Diego, CA: SPIE - The International Society for Optical Engineering, p. 72871Y (12 pp.).
17. Kornbluh RD, Pelrine R, Prahlad H, et al. Dielectric elastomers: Stretching the capabilities of energy harvesting. *MRS Bull* 2012; 37: 246–253.
18. Chiba S, Waki M, Kornbluh R, et al. Current status and future prospects of power generators using dielectric elastomers. *Smart Mater Struct* 2011; 20.
19. Anderson IA, Ieropoulos IA, McKay T, et al. Power for robotic artificial muscles. *IEEE/ASME Trans Mechatron* 2011; 16: 107–111.
20. Pelrine R, Kornbluh R, Pei Q, et al. Dielectric elastomer artificial muscle actuators: Toward biomimetic motion. In: *Smart Structures and Materials 2002: Electroactive polymer actuators and devices (EAPAD)*, 18–21 March 2002. San Diego, CA: SPIE, 2002, pp.126–137.
21. Jean-Mistral C, Basrour S and Chaillout JJ. Dielectric polymer: scavenging energy from human motion. In: *Electroactive polymer actuators and devices (EAPAD)*, 10 March 2008. San Diego, CA: SPIE - The International Society for Optical Engineering, pp.692716-1.
22. Jean-Mistral C and Basrour S. Scavenging energy from human motion with tubular dielectric polymer. In: *Electroactive polymer actuators and devices (EAPAD)*, 8 March 2010. San Diego, CA: SPIE - The International Society for Optical Engineering, p. 764209 (12 pp.).
23. Martins PALS, Natal Jorge RM and Ferreira AJM. A comparative study of several material models for prediction of hyperelastic properties: Application to silicone-rubber and soft tissues. *Strain* 2006; 42: 135–147.
24. Lochmatter P, Kovacs G and Michel S. Characterization of dielectric elastomer actuators based on a hyperelastic film model. *Sens Actuat A* 2007; 135: 748–757.
25. Brochu P, Li H, Niu X, et al. Factors influencing the performance of dielectric elastomer energy harvesters. In: TSoP-OIE (ed.) *Electroactive polymer actuators and devices (EAPAD)*, 8–10 March 2010. San Diego, CA: SPIE, pp.76422J-1 (12 pp.).
26. Liu L, Shouhua S, Kai Y, et al. The area of allowable states in Mooney-Rivlin type dielectric elastomer generators. In: *Electroactive polymer actuators and devices (EAPAD)*, 8 March 2010. San Diego, CA: SPIE - The International Society for Optical Engineering, p. 764238 (8 pp.).
27. Ogden RW. Large deformation isotropic elasticity - on the correlation of theory and experiment for incompressible rubberlike solids. *Proc Roy Soc Lond Ser A* 1972; 326: 565–584.
28. Wissler M and Mazza E. Modeling of a pre-strained circular actuator made of dielectric elastomers. *Sens Actuat A* 2005; 120: 184–192.
29. Graf C, Aust M, Maas J, et al. Simulation model for electro active polymer generators. In: *2010 10th IEEE international conference on solid dielectrics (ICSD 2010)*, 4–9 July 2010. Piscataway, NJ: IEEE, 2010, p. 4.
30. Graf C, Maas J and Schapeler D. Energy harvesting cycles based on electro active polymers. In: TSoP-OIE (ed.) *Electroactive polymer actuators and devices (EAPAD*, 8–11 March 2010. San Diego, CA: SPIE, pp.764217-1 (12 pp.).
31. Kofod G, Sommer-Larsen P, Kornbluh R, et al. Actuation response of polyacrylate dielectric elastomers. *J Intell Mater Syst Struct* 2003; 14: 787–793.

Appendix

Notation

C	capacitance (F)
E	electric field (V/m)
F_i	force in the principal directions (N)
I_i	invariants of the deformation tensor
p	hydrostatic pressure (Pa)
Q	charge (C)
V	voltage (V)
W	strain energy density function
x_{2avg}	theoretical average width due to parabola shaped edges in lateral direction (m)
x_i	extension in principal directions; (x_1 – axial, x_2 – lateral, x_3 – transverse) (m)
x_{i0}	initial length in principal directions (m)
ε	permittivity of the dielectric material (F/m)
κ	boundary constraint coefficient
λ_{2avg}	theoretical average stretch due to parabola-shaped edges in lateral direction
λ_i	stretch ratios in the principal directions
$\tilde{\lambda}$	equilibrium Maxwell stretch ratio; $\tilde{\lambda}_c$ at charge, $\tilde{\lambda}_d$ at discharge
$\tilde{\lambda}_i$	Maxwell stretch ratios in principle directions
σ_i	principal stresses (Pa)
σ_i^{MY}	principal stresses calculated using the modified Yeoh model (Pa)
σ_{iM}	stresses in principle directions which result from Maxwell stress (Pa)
σ_M	Maxwell stress (Pa)
$\forall$	volume of DE film (m^3)